

Mutual Antagonism of Target of Rapamycin and Calcineurin Signaling*

Received for publication, May 3, 2006, and in revised form, September 6, 2006. Published, JBC Papers in Press, September 7, 2006, DOI 10.1074/jbc.M604244200

Jose M. Mulet¹, Dietmar E. Martin, Robbie Loewith², and Michael N. Hall³

From the Biozentrum, University of Basel, Klingelbergstrasse 70, CH 4056 Basel, Switzerland

Growth and stress are generally incompatible states. Stressed cells adapt to an insult by restraining growth, and conversely, growing cells keep stress responses at bay. This is evident in many physiological settings, including for example, the effect of stress on the immune or nervous system, but the underlying signaling mechanisms mediating such mutual antagonism are poorly understood. In eukaryotes, a central activator of cell growth is the protein kinase target of rapamycin (TOR) and its namesake signaling network. Calcineurin is a conserved, Ca²⁺/calmodulin-dependent protein phosphatase and target of the immunosuppressant FK506 (tacrolimus) that is activated in yeast during stress to promote cell survival. Here we show yeast mutants defective for TOR complex 2 (TORC2) or the essential homologous TORC2 effectors, SLM1 and SLM2, exhibited constitutive activation of calcineurin-dependent transcription and actin depolarization. Conversely, cells defective in calcineurin exhibited SLM1 hyperphosphorylation and enhanced interaction between TORC2 and SLM1. Furthermore, a mutant SLM1 protein (SLM1^{ΔC14}) lacking a sequence related to the consensus calcineurin docking site (PxIxIT) was insensitive to calcineurin, and SLM1^{ΔC14} *slm2* mutant cells were hypersensitive to oxidative stress. Thus, TORC2-SLM signaling negatively regulates calcineurin, and calcineurin negatively regulates TORC2-SLM. These findings provide a molecular basis for the mutual antagonism of growth and stress.

TOR⁵ is a serine/threonine kinase and a central controller of cell growth. TOR is found in two structurally and functionally distinct, evolutionarily conserved protein complexes, TORC1 and TORC2 (1–3). TORC1 is rapamycin-sensitive and controls several growth-related processes including transcription, translation, ribosome biogenesis, nutrient transport, and autophagy in response to nutrient, energy, and (in metazoans) growth factor signals (3). TORC2 is rapamycin-insensitive and

controls polarization of the actin cytoskeleton via a ROM2-RHO-PKC1-MPK1/SLT2 effector pathway (4, 5). Thus, TOR via its two complexes integrates temporal and spatial control of cell growth.

In the yeast *Saccharomyces cerevisiae*, calcineurin promotes cell survival upon environmental stress (6). In response to a stress-induced increase in cytoplasmic calcium, calcineurin dephosphorylates and activates several cytoplasmic targets. The calcineurin docking site in target proteins consists of the consensus sequence PxIxIT. The best characterized calcineurin target in yeast is the transcription factor CRZ1/TCN1/HAL8 (7–9). Dephosphorylated CRZ1 translocates into the nucleus and activates target genes containing a calcineurin-dependent response element. These genes are involved mainly in ion homeostasis, vesicular transport, and cell wall maintenance. Independent of transcription, calcineurin also mediates stress-induced depolarization of the actin cytoskeleton and a delay in the G₂–M transition of the cell cycle (10, 11). Calcineurin is a heterodimer composed of a positive regulatory subunit (CNB1) and in *S. cerevisiae*, one of the redundant catalytic subunits CNA1 and CNA2.

Cells respond to environmental stress by down-regulating energy demanding growth processes and up-regulating survival processes. How do cells counter-regulate growth and stress responses? A functional interaction between calcineurin and TOR has been suggested by a two-hybrid interaction between CNA (CNA1 or CNA2) and the TORC2 phosphorylation substrates SLM1 and SLM2 (12). The homologous SLM1 and SLM2 are redundant, essential proteins that control polarization of the actin cytoskeleton by an unknown mechanism (13, 14). In this study we show that TORC2 and calcineurin inhibit each other via the SLM proteins. Our findings provide a molecular mechanism for the mutual antagonism of growth-promoting and growth-inhibiting signaling pathways. Furthermore, we show that TORC2 controls transcription and has a pivotal role in the negative regulation of calcineurin-dependent stress signaling, in addition to controlling organization of the actin cytoskeleton.

EXPERIMENTAL PROCEDURES

Strains, Plasmids, and Media—The *S. cerevisiae* strains and plasmids used in this study are listed in Table 1. All strains are isogenic derivatives of TB50 or JK9-3d. Medium (YPD/YPGal) was prepared as described previously (15, 16). YPD containing 0.2 M CaCl₂ was prepared by adding the required volume of a 1 M stock of CaCl₂ to 1.25-fold concentrated, autoclaved YPD. FK506 was added to a final concentration of

* The costs of publication of this article were defrayed in part by the payment of page charges. This article must therefore be hereby marked "advertisement" in accordance with 18 U.S.C. Section 1734 solely to indicate this fact. The amino acid sequence of this protein can be accessed through NCBI Protein Database under NCBI accession number GSE1814.

¹ Supported by the Spanish Ministry of Science and Education (MEC) and by a grant from the European Union Research Network, "Adaptation to Changing Nutritional Environments."

² Present address: Dept. of Molecular Biology, University of Geneva, 30 quai Ernest-Ansermet, CH 1211, Geneva 4, Switzerland.

³ Supported by the Swiss National Science Foundation and the Canton of Basel. To whom correspondence should be addressed. Tel.: 41-61-267-2150; Fax: 41-61-267-2148; E-mail: M.Hall@unibas.ch.

⁴ The abbreviations used are: TOR, target of rapamycin; HA, hemagglutinin; wt, wild type; TAP, tandem affinity purification.

TABLE 1

All strains are *S. cerevisiae*. Unless otherwise indicated, all the strains were constructed for this study

Strain	Genotype	Source
JK9-3da	MATa <i>leu2-3,112 ura3-52 trp1 his4 rme HMLa</i>	
JM229	TB50a <i>CNA1-3HA-[His3MX6]</i>	
JM256	TB50a <i>crz1::HIS3</i>	
JM259	TB50a <i>CNA1-3HA-[His3MX6] SLM1-13myc-[kanMX6]</i>	
JM262	TB50a <i>CRZ1-13myc-[His3MX6]</i>	
JM270	TB50a <i>[His3MX6]-GAL1p-SLM2 <i>slm1::kanMX6</i> CRZ1-13myc-[His3MX6]</i>	
JM271	TB50a <i>[His3MX6]-GAL1p-SLM2 <i>slm1::kanMX6</i> <i>crz1::HIS3</i></i>	
JM304	TB50a <i>cnb1::His3MX6</i>	
JM316	TB50a <i>cnb1::His3MX6</i>	
JM321	TB50a <i>[His3MX6]-GAL1p-AVO3 <i>crz1::HIS3</i></i>	
JM324	TB50a <i>[His3MX6]-GAL1p-AVO3 CRZ1-13myc-[His3MX6]</i>	
JM333	TB50a <i>SLM1-TAP-[kanMX6] <i>cnb1::His3MX6</i></i>	
JM338	TB50a <i>[His3MX6]-GAL1p-TOR2 <i>crz1::HIS3</i></i>	
JM340	TB50a <i>[His3MX6]-GAL1p-TOR2 CRZ1-13myc-[His3MX6]</i>	
JM345	TB50a <i>[His3MX6]-GAL1p-TOR2</i>	
JM347	TB50a <i>[His3MX6]-GAL1p-AVO3</i>	
JM474	TB50a <i>[His3MX6]-GAL1p-SLM2 <i>slm1::kanMX6</i> <i>cnb1::His3MX6</i></i>	
JM481	TB50a <i>AVO3-3HA-[kanMX6] SLM1-13myc-[kanMX6] <i>cnb1::His3MX6</i></i>	
JM491	TB50a <i>SLM1-13myc-[kanMX6] CNA1-3HA-[His3MX6] <i>cnb1::His3MX6</i></i>	
JM501	TB50a <i>[His3MX6]-GAL1p-TOR2 <i>cnb1::His3MX6</i></i>	
JM597	TB50a <i>SLM1^{ΔC14}-TAP-[His3MX6]</i>	
JM611	TB50a <i>SLM1^{ΔC14}-TAP-[His3MX6] <i>slm2::kanMX6</i></i>	
JM624	TB50a <i>SLM1^{ΔC14}-13myc-[His3MX6] CNA1-3HA-[His3MX6] <i>cnb1::His3MX6</i></i>	
JM626	TB50a <i>SLM1^{ΔC14}-13myc-[His3MX6] AVO3-3HA-[kanMX6]</i>	
JM712	TB50a <i>SLM1^{ΔC14}-TAP-[His3MX6] <i>cnb1::His3MX6</i></i>	
JM717	TB50a <i>SLM1^{ΔC14}-TAP-[His3MX6] <i>crz1::HIS3</i></i>	
RL42-1c	TB50a <i>AVO3-3HA-[kanMX6]</i>	
RL136-1a	TB50a <i>slm2::kanMX6</i>	
RL146-7d	TB50a <i>SLM1-13myc-[kanMX6]</i>	
RL164-2b	TB50a <i>AVO3-3HA-[kanMX6] SLM1-13myc-[kanMX6]</i>	
RL202-5a	TB50a <i>[His3MX6]-GAL1p-SLM2 <i>slm1::kanMX6</i></i>	
RL209	TB50a <i>SLM1-TAP-[kanMX6]</i>	
SH100	JK9-3da <i>tor2::ADE2-3/YCplac111::TOR2</i>	Ref. 19
SH121	JK9-3da <i>tor2::ADE2-3/YCplac111::tor2-21^{ts}</i>	Ref. 19
TB50a	JK9-3da <i>HIS4 his3</i>	Hall lab.

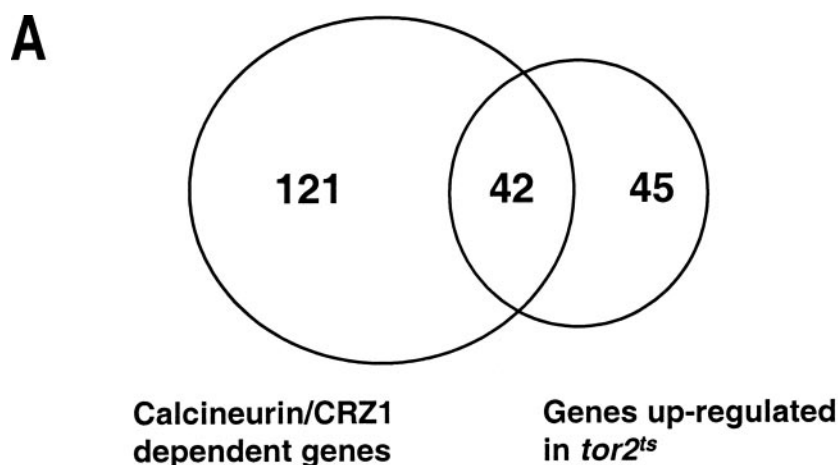
2 μg/ml from a 1 mg/ml stock in 90% ethanol-10% Tween 20. FK506 treatment was for 30 min. H₂O₂ was added from a 30% commercial solution (Fluka) to autoclaved YPD agar medium prior to solidification to a final concentration of 5 mM. For TOR2-, AVO3-, and SLM2-depletion experiments, YPGal cultures of logarithmically growing cells, conditionally expressing the corresponding genes from the *GAL1* promoter, were inoculated into YPD medium and incubated with aeration for 15 (TOR2 or AVO3 depletion) or 6 h (SLM2 depletion). The long incubation times reflect the amount of time required to deplete the proteins in question (17). PCR cassettes were used to generate gene deletions and epitope tags in the genome as described previously (18). An SLM mutant lacking the PxIXIT-related, putative calcineurin docking site was constructed by replacing the C-terminal 14 amino acids of SLM1 with a Myc or TAP tag in the genome as described above.

RNA Isolation, Microarray, and Northern Blot Analysis—For the microarray experiment, *S. cerevisiae* strains SH100 and SH121 (19) were grown at nonpermissive temperature (37 °C) for 6 h, as described (20). Total RNA was extracted using a hot phenol method essentially as described (21). Affymetrix™ S98 Yeast Genome GeneChips, containing 6,400 *S. cerevisiae* (S288C strain) genes, were used. Two independent RNA preparations were used for each strain. Quantity and quality of total RNA were determined by capillary electrophoresis on a RNA6000 Bioanalyzer (Agilent Technologies). Synthesis of cDNA, *in vitro* transcription of biotin-labeled cRNA, microarray hybridization, washing, and staining procedures were carried out according to standard protocols as recommended by

the manufacturer (Affymetrix). Data normalization was performed using the Robust Multi-array Analysis algorithm as implemented in GeneSpring 7.2 software. For Northern blot analysis, probe synthesis was performed by PCR using digoxigenin-modified dUTP, and subsequent Northern blot analysis was performed according to the manufacturer's protocol (digoxigenin labeling and detection, Roche).

Coimmunoprecipitation, TAP Purification, and Immunoblotting—Coimmunoprecipitations and the TAP pulldown assays were performed as described (17). HA- and Myc-tagged proteins were precipitated or detected with mouse anti-HA antibody (clone 12CA5) or mouse anti-Myc antibody (clone 9E10). Phospho-SLM1-TAP was detected by immunoblotting with anti-phosphothreonine (Q7, Qiagen) and anti-phosphoserine (Q5, Qiagen) antibodies. Total SLM1-TAP was detected with anti-TAP (protein A) antibody. Horseradish peroxidase-conjugated anti-mouse antibody and ECL reagents were used for immunoblots (Amersham Biosciences). Proteins coprecipitating in TAP pulldowns were excised from a 5–20% gradient gel and identified by mass spectrometry as described (1).

In Vitro Calcineurin Assay—Phospho-SLM1-TAP was purified for use as a calcineurin substrate by TAP pull down from an extract prepared from JM333 yeast cells (*cnb1*) as described (17) but using TL buffer (40 mM Tris-HCl, pH 7.5, 100 mM KCl, 1 mM MgCl₂, 250 mM sorbitol, 1 mM dithiothreitol, 0.1% Nonidet P-40) instead of phosphate-buffered saline buffer. The slurry of IgG beads containing SLM1-TAP was washed with CP buffer (50 mM Tris-HCl, pH 7.5, 1 mM MgCl₂, 1 mM dithiothreitol) containing protease inhibitors. The calcineurin reaction



B

ORF	NAME	FUNCTION
<i>YAR036w</i>	<i>PRM9</i>	Pheromone regulated membrane protein
<i>YBR005w</i>	<i>RCR1</i>	Endoplasmic reticulum membrane protein
<i>YBR296c</i>	<i>PHO89</i>	Na/Pi symporter
<i>YDL010w</i>		Unknown
<i>YDL234c</i>	<i>GYP7</i>	GTPase-activating protein
<i>YDR210w</i>		Unknown
<i>YEL060c</i>	<i>PRB1</i>	Vacuolar protease B
<i>YER185w</i>		Unknown
<i>YGL006w</i>	<i>PMC1</i>	Ca ²⁺ -ATPase
<i>YGR213C</i>	<i>RTA1</i>	Involved in 7-amincholesterol resistance
<i>YHR071w</i>	<i>PCL5</i>	PHO85 cyclin
<i>YHR097c</i>		Unknown
<i>YHR138c</i>		Homologous to PBI2
<i>YHR139c</i>	<i>SPS100</i>	Sporulation specific cell wall maturation protein
<i>YJL016w</i>		Unknown
<i>YJL165c</i>	<i>HAL5</i>	Protein kinase similar to NPR1
<i>YKL001c</i>	<i>MET14</i>	Adenylylsulfate kinase
<i>YKL159c</i>	<i>RCN1</i>	Regulator of calcineurin
<i>YLL057c</i>	<i>JLP1</i>	Fe(II)-dependent sulfonate/alpha-ketoglutarate dioxygenase
<i>YLR054c</i>	<i>OSW2</i>	Hypothetical protein involved in spore wall assembly.
<i>YLR099c</i>	<i>ICT1</i>	Involved in drug tolerance
<i>YLR120c</i>	<i>YPS1</i>	GPI-anchored aspartic protease
<i>YLR136c</i>	<i>TIS11</i>	Zinc finger protein
<i>YLR142w</i>	<i>PUT1</i>	Proline oxidase
<i>YLR194c</i>		Hypothetical cell wall protein
<i>YLR327c</i>	<i>RBP9</i>	Unknown
<i>YLR414c</i>		Unknown
<i>YMR095c</i>	<i>SNO1</i>	Involved in pyridoxine metabolism. Unconfirmed function
<i>YMR096w</i>	<i>SNZ1</i>	Involved in vitamin B6 biosynthesis
<i>YMR107w</i>	<i>SPG4</i>	Involved in high temperature survival during stationary phase
<i>YMR316w</i>	<i>DIA1</i>	Involved in pseudohyphal growth
<i>YNL092w</i>		Putative S-adenosylmethionine-dependent methyltransferase
<i>YNR064c</i>		Epoxide hydrolase
<i>YOL016c</i>	<i>CMK2</i>	Calmodulin dependent protein kinase
<i>YOL084w</i>	<i>PHM7</i>	Unknown
<i>YOL158c</i>	<i>ENB1</i>	Ferric enterobactin transporter
<i>YOR019w</i>		Unknown
<i>YOR036w</i>	<i>PEP12</i>	t-SNARE
<i>YOR134w</i>	<i>BAG7</i>	GTPase activating protein
<i>YOR220w</i>		Unknown
<i>YOR338w</i>		Unknown
<i>YOR385w</i>		Unknown

FIGURE 1. **Microarray analysis of a *tor2* mutant defective in TORC2.** A, summary of DNA microarray analysis. Genes induced in a calcineurin/CRZ1-dependent manner (24) and those induced in a *tor2^{ts}* mutant are compared. B, names and brief descriptions of the genes included in the diagram intersection in A. Raw microarray data files can be found in the NCBI GEO repository under the series number GSE1814.

was performed in a total volume of 100 μ l in CP buffer containing 500 units of recombinant human calcineurin (Calbiochem) and 2600 units of calmodulin (Sigma) as described (22). Where indicated, CaCl₂ and EGTA were added to a final concentration of 40 and 10 mM, respectively. Phosphatase reactions were incubated at 30 °C for 30 min. Phospho-SLM1-TAP and total SLM1-TAP were detected as described above.

Microscopy—Fluorescence microscopy and indirect immunofluorescence imaging on whole fixed cells were performed as

described (23). An anti-Myc (9E10) antibody was used to visualize CRZ1-Myc. Control experiments with wild type cells showed that the unspecific signal was negligible in our strain. For actin cytoskeleton or DNA staining, we used a modification of the method described in (1), eliminating the phosphate buffer to avoid calcium phosphate precipitation. Cells from the indicated YPD cultures were fixed in formaldehyde (3.7%) and stained with tetramethyl rhodamine isothiocyanate-phalloidin (Sigma) to visualize actin or 4',6-diamidino-2-phenylindole to stain DNA and visualize nuclei. Actin cytoskeleton organization was assessed in several hundred cells as described (19).

RESULTS

TORC2 Negatively Controls Calcineurin-dependent Transcription—TORC2, because of its rapamycin insensitivity, is less well characterized than TORC1. To further investigate TORC2, we performed a genome-wide transcriptome analysis on an *S. cerevisiae* strain (SH121) containing the thermosensitive *tor2-21* (*tor2^{ts}*) allele (19). This strain is defective for TORC2 but not for TORC1 (1, 17). At nonpermissive temperature, ~90 genes were up-regulated (≥ 2 -fold induction), and no genes were significantly down-regulated in the *tor2^{ts}* mutant, compared with wild type (Fig. 1). This suggests that TORC2 controls transcription, mainly negatively. Further analysis revealed that ~50% of the genes inhibited by TORC2 overlapped with a set of genes, the expression of which was dependent on calcineurin and CRZ1 for expression (≥ 5.5 -fold induction upon calcineurin activation). These findings suggest that TORC2 inhibits calcineurin and CRZ1.

To determine whether TORC2 indeed inhibits CRZ1, we examined CRZ1-dependent transcription directly in a *tor2* mutant and in a mutant defective for the TORC2-specific subunit AVO3. Transcripts corresponding to the CRZ1 target genes *CMK2*, *DIA1*, *YLR194c*, and *YOR385w* were probed by Northern analysis in strains conditionally expressing *TOR2* or *AVO3* from the galactose-inducible and

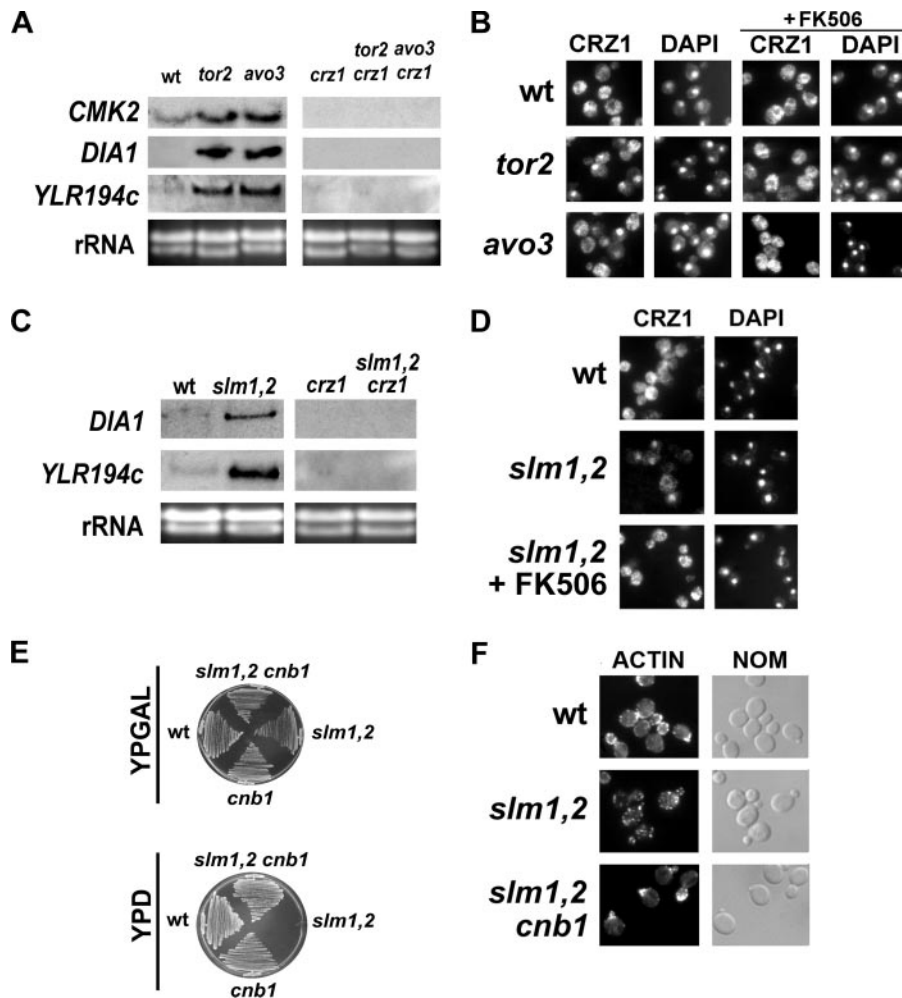


FIGURE 2. TORC2 negatively regulates calcineurin and CRZ1 via the SLM proteins. *A*, CRZ1-dependent transcription is constitutively activated in TORC2 mutants. Transcripts of the indicated CRZ1 target genes were visualized in the indicated strains, wt (TB50a), *tor2* (JM345), *avo3* (JM347), *crz1* (JM256), *tor2 crz1* (JM338), *avo3 crz1* (JM321), by Northern analysis. *B*, the calcineurin-dependent transcription factor CRZ1 localizes to the nucleus in *tor2* and *avo3* mutant. This constitutive localization is abolished upon inhibition of calcineurin by addition of FK506 to cells. CRZ1 localization (CRZ1) was examined in the following strains: wt (JM262), *tor2* (JM340), and *avo3* (JM324). In all cases, a monoclonal anti-Myc antibody was used as a primary antibody for indirect immunofluorescence. DNA was stained with 4',6-diamidino-2-phenylindole to visualize nuclei. *C*, CRZ1-dependent transcription is constitutively activated in *slm1,2* mutants. Transcripts of the indicated CRZ1 target genes were visualized in the indicated strains, wt (TB50a), *slm1,2* (RL202-5a), *crz1* (JM256), *slm1,2 crz1* (JM271), by Northern analysis. *D*, the calcineurin-dependent transcription factor CRZ1 localizes to the nucleus in a *slm1,2* mutant. This constitutive localization is abolished upon inhibition of calcineurin by addition of FK506 to cells. CRZ1 localization (CRZ1) was examined in a wt (JM262) and in a *slm1,2* mutant (JM270). In all cases, a monoclonal anti-Myc antibody was used as a primary antibody for indirect immunofluorescence. DNA was stained with 4',6-diamidino-2-phenylindole to visualize nuclei. *E*, deletion of the regulatory subunit of calcineurin (CNB1) suppresses the lethality of a conditional *slm1,2* mutant. Strain *slm1,2 cnb1* (JM474) was constructed by crossing strain *slm1,2* (RL202-5a) with *cnb1* (JM316) and selecting strains with the appropriate markers. Growth of the indicated strains was tested on permissive (YPGal) and nonpermissive (YPD) medium by incubating the different plates for 3 days at 30 °C. *F*, *CNB1* mutation suppresses the actin depolarization phenotype of a *slm1 slm2* double mutant (*slm1,2*). Strains described in *E* were grown in restrictive (YPD) medium to mid-logarithmic phase, fixed, and stained for F-actin using rhodamine-phalloidin (ACTIN). Cells were visualized using Nomarski optics (NOM).

glucose-repressible *GAL1* promoter. Strains conditionally expressing *TOR2* or *AVO3* were used, instead of strains containing a thermosensitive *tor2* or *avo3* allele, to avoid potential complications because of heat stress activation of CRZ1. The CRZ1 target genes were induced upon depletion of TOR2 or AVO3 and in the absence of any other stress (Fig. 2A; data not shown for *YOR385w*). The CRZ1 dependence of the examined transcripts was determined by deleting *CRZ1* in the *tor2* and *avo3* strains

(Fig. 2A). We also observed calcineurin-dependent response element (CDRE)-dependent expression of *lacZ* upon TOR2 or AVO3 depletion (data not shown). These experiments confirm the results of the transcriptome analysis with the *tor2^{ts}* mutant and indicate that the expression changes observed with the *tor2^{ts}* mutant are not necessarily because of heat stress. Thus, TORC2 inhibits CRZ1-dependent transcription under normal growth conditions, *i.e.* in the absence of stress.

Calcineurin dephosphorylates CRZ1 and thereby triggers nuclear localization and activation of CRZ1 (25). To investigate whether TORC2 regulates calcineurin, we examined CRZ1 localization in the *tor2* and *avo3* mutants by indirect immunofluorescence on whole fixed cells (Fig. 2B). In both *tor2* and *avo3* mutant cells, CRZ1 was exclusively (15–20% of cells) or mainly (45–50% of cells) nuclear, whereas in wild type cells CRZ1 was exclusively or mainly cytoplasmic. Thus, TORC2 inhibits nuclear accumulation of CRZ1. To investigate the calcineurin-dependence of CRZ1 nuclear localization in the *tor2* and *avo3* mutants, cells were treated with the calcineurin inhibitor FK506. A short treatment (30 min) with FK506 restored cytoplasmic localization of CRZ1 in *tor2* and *avo3* cells (Fig. 2B). Similar suppression of the CRZ1 localization defect was obtained upon deletion of *CNB1* encoding the positive regulatory subunit of calcineurin (data not shown). Thus, CRZ1 nuclear localization in the *tor2* and *avo3* mutants was calcineurin-dependent. The above findings suggest that TORC2 negatively regulates calcineurin. However, these experiments do not

distinguish whether the TORC2 inhibits calcineurin directly or indirectly.

TORC2 Inhibits Calcineurin via the SLM Proteins—The observation that the TORC2 substrates SLM1 and SLM2 interact with the catalytic subunit of calcineurin (CNA1 or CNA2), as revealed by a genome-wide two-hybrid study (12), suggests that TORC2 inhibits calcineurin via the SLMs. To investigate this possibility, we examined CRZ1-dependent transcription and CRZ1 localization in a *slm1 slm2* double mutant (*slm1,2*).

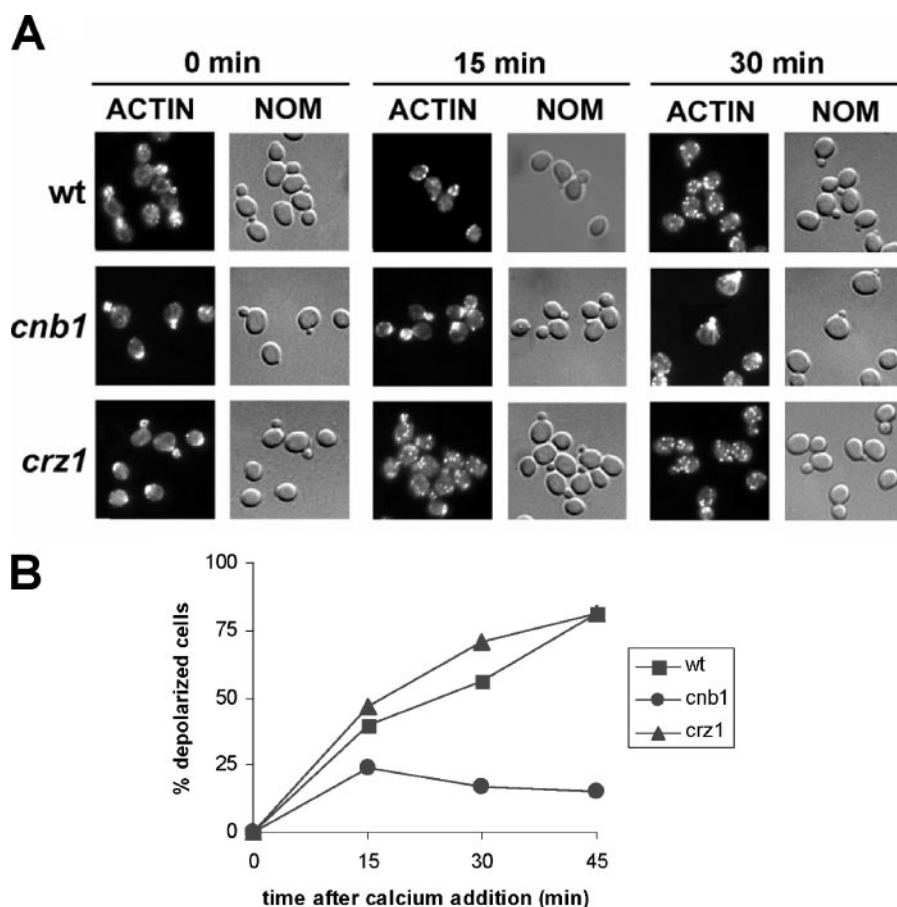


FIGURE 3. Calcineurin mediates depolarization of the actin cytoskeleton independently of CRZ1. *A*, wt (TB50a), *cnb1* (JM304), and *crz1* (JM256) cells were grown in YPD medium until mid-logarithmic phase and then transferred to fresh medium containing 0.2 M CaCl₂ to activate calcineurin. At the indicated times, aliquots were removed, fixed, and stained for F-actin using rhodamine-phalloidin (ACTIN). Cells were visualized using Nomarski optics (NOM). *B*, quantitation of the actin depolarization induced by calcium. Small to medium budded cells (≈ 200) of wild type (squares), *cnb1* (circles), and *crz1* (triangles) strains were scored for their actin polarization state. Similar results were obtained in three separate experiments.

Because the SLMs are essential, strains containing a *SLM1* deletion and conditionally expressing *SLM2* from the *GAL1* promoter were used for these experiments. In a *slm1,2* mutant, CRZ1 accumulated in the nucleus in a calcineurin-dependent (FK506 sensitive) manner and activated transcription of target genes (data not shown for *YOR385w*) even in the absence of stress (Fig. 2, *C* and *D*). In addition, inhibition of calcineurin by treatment with FK506 or by deletion of *CNB1* suppressed the growth and actin defects of a *slm1,2* mutant (Fig. 2, *E* and *F*). Thus, calcineurin appears to be constitutively active in a *slm1,2* mutant, like in TORC2 mutants (*tor2* and *avo3*) and the cause of lethality of a *slm1,2* mutation. These observations suggest that TORC2 negatively regulates calcineurin via the SLMs. Furthermore, the suppression of the *slm1,2* actin defect by *CNB1* deletion or by FK506 treatment suggests that the SLMs mediate actin polarization via inhibition of calcineurin.

Interestingly, inhibition of calcineurin did not suppress the lethality of a *tor2* or *avo3* mutation (data not shown). Furthermore, multicopy *ROM2* or *RHO2*, strong suppressors of *tor2* or *avo3* lethality (1, 4), failed to suppress either the growth defect or the CRZ1 nuclear localization phenotype of the *slm1,2* mutant (data not shown) (14). Overexpression of *ROM2* or

RHO2 also failed to suppress the CRZ1 nuclear localization phenotype of the *tor2* mutant (data not shown). These observations suggest that TORC2 signals via SLM-calcineurin and ROM2-RHO-PKC-MPK1/SLT2 separately.

Calcineurin Antagonizes TORC2-SLM Signaling—TORC2 positively controls polarization of the actin cytoskeleton. In contrast, activation of calcineurin causes depolarization of the actin cytoskeleton (Fig. 2*F* and Fig. 3). Furthermore, calcineurin causes depolarization of the actin cytoskeleton independently of CRZ1 (Fig. 3). These observations suggest that calcineurin may antagonize the ability of TORC2 to signal via the SLMs. To address this suggestion, we first investigated whether calcineurin (CNA1) interacts with SLM1 as suggested previously by a genome-wide two-hybrid analysis (12). Our efforts to detect, by coimmunoprecipitation, an SLM1-CNA1 interaction in a wild type strain were unsuccessful. As this could be because of CNA1 dephosphorylating and thereby releasing SLM1, we then investigated an SLM1-CNA1 interaction under conditions in which calcineurin was inactive. Inhibition of calcineurin by a *cnb1* mutation or by treatment of cells with FK506 indeed resulted in detection of an

SLM1-CNA1 interaction (Fig. 4*A*) (data not shown for FK506). To study further the SLM1-CNA1 interaction, we examined whether SLM1 contained a PxIxIT calcineurin docking site. Although we did not detect a consensus PxIxIT sequence, a related sequence (PNIYIQ) was detected in the C-terminal 14 amino acids of SLM1 (PNIYIQ TPINDFKS). To determine whether this PxIxIT-related sequence is a calcineurin docking site, the C-terminal 14 amino acids of SLM1 were deleted, and the truncated protein (SLM1^{ΔC14}) was assayed by coimmunoprecipitation for interaction with CNA1. SLM1^{ΔC14} failed to interact with CNA1 even upon inhibition of calcineurin (Fig. 4*A*), suggesting that the PxIxIT-related sequence in SLM1 was a calcineurin binding site. The SLM1^{ΔC14} mutant protein was functional other than in its ability to interact with CNA1 because a *SLM1*^{ΔC14} *slm2* double mutant grew like a wild type strain under standard growth conditions, unlike the *slm1 slm2* double mutant (*slm1,2*), which was nonviable (data not shown). The above findings indicate that calcineurin interacts directly with SLM1. Interestingly, the observation that SLM1^{ΔC14} is functional despite its inability to interact with calcineurin suggests that SLM1 has a function independent of its direct interaction with calcineurin.

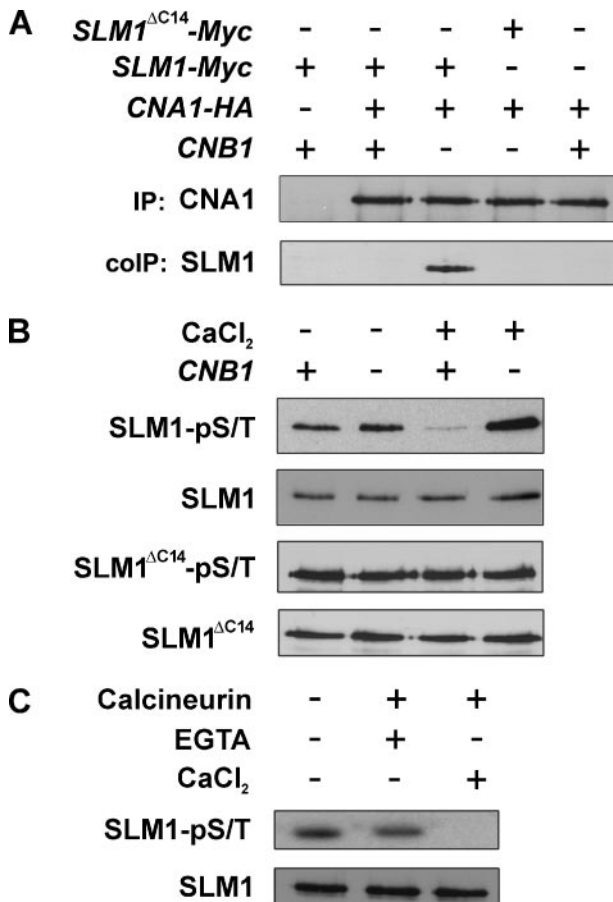


FIGURE 4. SLM1 is a target of calcineurin. A, CNA1 and SLM1 interact in a calcineurin-sensitive manner. Cells expressing epitope-tagged CNA1 (*CNA1-HA*) (JM229), SLM1 (*SLM1-Myc*) (RL146-7d), co-expressing both tagged proteins (JM259 and JM491) or co-expressing epitope-tagged CNA1 with an epitope-tagged version of SLM1 (*SLM1^{ΔC14}*) lacking the C-terminal 14 amino acids (*SLM1^{ΔC14}-Myc*) (JM624), were grown to mid-logarithmic phase, harvested, lysed, and cell extracts were subjected to immunoprecipitation with anti-HA (IP: CNA1). Immunoprecipitates were probed with anti-Myc to detect coimmunoprecipitated SLM1 protein (coIP: SLM1). CNA1 and SLM1 interact only in a *cnb1* mutant. B, calcineurin dephosphorylates SLM1 *in vivo*. SLM1-TAP (RL209), SLM1-TAP *cnb1* (JM333), SLM1^{ΔC14}-TAP (JM597), and SLM1^{ΔC14}-TAP *cnb1* (JM712) cells were grown to mid-logarithmic phase and either mock-treated or treated with 200 mM CaCl₂ for 10 min. Cells were harvested and subjected to protein extraction and TAP purification, SDS-PAGE, and immunoblotting. The immunoblotting was performed with an anti-TAP (protein A) antibody to detect total SLM1-TAP (SLM1) or SLM1^{ΔC14}-TAP (SLM1^{ΔC14}) or with a mixture of commercial antibodies against phosphorylated serine and phosphorylated threonine to detect phospho-SLM1-TAP (SLM1-pS/T) or phospho-SLM1^{ΔC14}-TAP (SLM1^{ΔC14}-pS/T) (see "Experimental Procedures"). C, calcineurin dephosphorylates phospho-SLM1 *in vitro*. Phospho-SLM1-TAP (SLM1-pS/T) was purified from *cnb1* cells (JM333) and treated with recombinant calcineurin (plus calmodulin), CaCl₂, and EGTA as indicated and described under "Experimental Procedures." SLM1-pS/T and total SLM1-TAP (SLM1) were detected as described above.

We detected a physical interaction between SLM1 and the calcineurin catalytic subunit CNA1 but only in the absence of calcineurin activity (see above). The observation that only inactive CNA1 forms a stable complex with SLM1 suggests that calcineurin may dephosphorylate SLM1. To investigate whether calcineurin dephosphorylates SLM1, we examined the phosphorylation status of SLM1 and SLM1^{ΔC14} in wild type and *cnb1* mutant cells, treated and untreated with calcium. Affinity (TAP)-tagged SLM1 and SLM1^{ΔC14} were purified and then probed with anti-phosphoSer/Thr antibody. SLM1 was hyper-

phosphorylated in the *cnb1* mutant compared with in a wild type strain (Fig. 4B). SLM1^{ΔC14}, consistent with its inability to interact with calcineurin, was hyperphosphorylated under all conditions examined (Fig. 4B). These findings suggest that calcineurin dephosphorylates SLM1 *in vivo*. Furthermore, recombinant calcineurin (plus calmodulin) dephosphorylated purified phospho-SLM1-TAP *in vitro* (Fig. 4C). This observation, combined with the previous observation that SLM1 physically interacts with calcineurin, suggests that calcineurin dephosphorylates SLM1 directly.

To investigate the functional consequence of SLM1 hyperphosphorylation, we examined the interaction between SLM1 and TORC2 in wild type and *cnb1* mutant cells. The TORC2-SLM interaction is weak (13, 14) and undetectable in our experimental conditions, as assayed by coimmunoprecipitation of SLM1 with AVO3 or TOR2 (Fig. 5, A and B). Inhibition of calcineurin, upon introduction of a *cnb1* mutation or treatment of cells with FK506, significantly enhanced the binding of SLM1 to both AVO3 and TOR2 (Fig. 5, A and B) (data not shown for FK506). Furthermore, the SLM1^{ΔC14} variant that was unable to bind calcineurin also exhibited enhanced binding to AVO3 and TOR2 (Fig. 5, A and B). Thus, calcineurin both dephosphorylates SLM1 and inhibits the TORC2-SLM1 interaction, suggesting that calcineurin antagonizes TORC2-SLM signaling.

To investigate further the physiological significance of SLM1 phosphorylation, we performed a more extensive phenotypic analysis of the *SLM1^{ΔC14} slm2* mutant, which grew like wild type under normal growth conditions. The *SLM1^{ΔC14} slm2* mutant was exposed to various stress conditions, including heat (37 °C), cold (15 °C), osmotic (1.8 M sorbitol or 1 M NaCl), lithium (0.3 M), calcium (0.2 M CaCl₂), and oxidative (5 mM H₂O₂) stress. The *SLM1^{ΔC14} slm2* was hypersensitive specifically to oxidative stress, as evidenced by a growth defect only in the presence of H₂O₂ (Fig. 5C and data not shown). Thus, phosphorylated SLM1 prevents the cellular response to oxidative stress, suggesting that TORC2-SLM signaling inhibits the response to this stress. In other words, calcineurin inhibits the ability of TORC2-SLM signaling to keep the response to oxidative stress at bay. A *crz1* mutation failed to confer hypersensitivity to oxidative stress, indicating that TORC2-SLM2 signaling inhibited the response to oxidative stress independently of CRZ1-dependent transcription.

DISCUSSION

We have presented evidence that TORC2-SLM signaling inhibits calcineurin, and conversely, calcineurin inhibits TORC2-SLM signaling. According to this model (Fig. 6), TORC2 phosphorylates the SLM proteins (13, 14) and thereby inhibited calcineurin and calcineurin-mediated events such as actin cytoskeleton depolarization and CRZ1-dependent transcription. Conversely, calcineurin dephosphorylates the SLMs and thereby inhibits TORC2-SLM signaling to the oxidative stress response and possibly other effectors. Thus, TORC2 and calcineurin are mutually antagonistic. The logic of this mutual antagonism may be the need to cope with the conflicting states of growth and stress. TORC2 prevents the calcineurin-activated stress response during favorable conditions, and conversely, calcineurin prevents TOR-mediated growth during

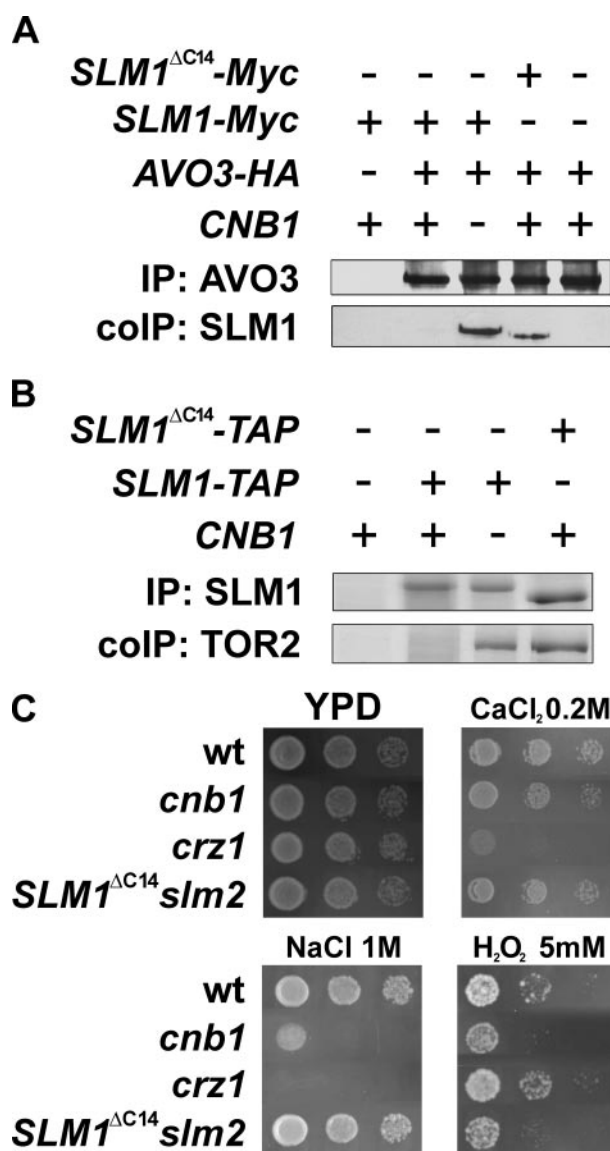


FIGURE 5. Calcineurin inhibits the interaction between TORC2 and SLM1. *A*, interaction of TORC2 component AVO3 with SLM1 is calcineurin-sensitive. Cells expressing epitope-tagged AVO3 (*AVO3-HA*) (RL42-1c), SLM1 (*SLM1-Myc*) (RL146-7d), both (RL164-2b and JM491), or AVO3 and an epitope-tagged version of SLM1^{ΔC14} (*SLM1^{ΔC14}-Myc*) (JM626) were grown to mid-logarithmic phase, harvested, and lysed, and cell extracts were subjected to immunoprecipitation with anti-HA (IP: AVO3). Immunoprecipitates were probed with anti-Myc to detect coimmunoprecipitated SLM1 protein (coIP: SLM1). AVO3 and SLM1 interacted in a *cnb1* mutant, or when the 14 C-terminal residues of SLM1 were deleted. *B*, interaction of TOR2 with SLM1 is calcineurin-sensitive. Lysates from wild type (mock purification), SLM1-TAP (RL209), SLM1-TAP *cnb1* (JM333), and SLM1^{ΔC14}-TAP (JM597) strains were subjected to TAP purification (IP: SLM1). Proteins were separated in a 5–20% gradient gel and stained with coomassie. TOR2 (coIP: TOR2) and SLM1 were identified by mass spectrometry. TOR2 and SLM1 interacted in a *cnb1* mutant, or when the C terminus of SLM1 was truncated. *C*, *SLM1^{ΔC14} slm2* is sensitive to hydrogen peroxide. The indicated strains wt (RL209), *cnb1* (JM333), *crz1* (JM171), and *SLM1^{ΔC14} slm2* (JM611) were grown to saturation in rich medium, serially diluted in water (1/10, 1/100, and 1/1000), and spotted on YPD agar or YPD agar containing the indicated compound. Growth was recorded after 48 to 72 h of incubation at 30 °C.

stress. The inhibition of calcineurin by TORC2 also allows a cell to resume growth after a stress has been overcome. Finally, another noteworthy aspect of the model (Fig. 6), which is suggested by our finding that a *cnb1* mutation suppresses the *slm1,2* actin defect, is that the SLMs mediate actin cytoskeleton

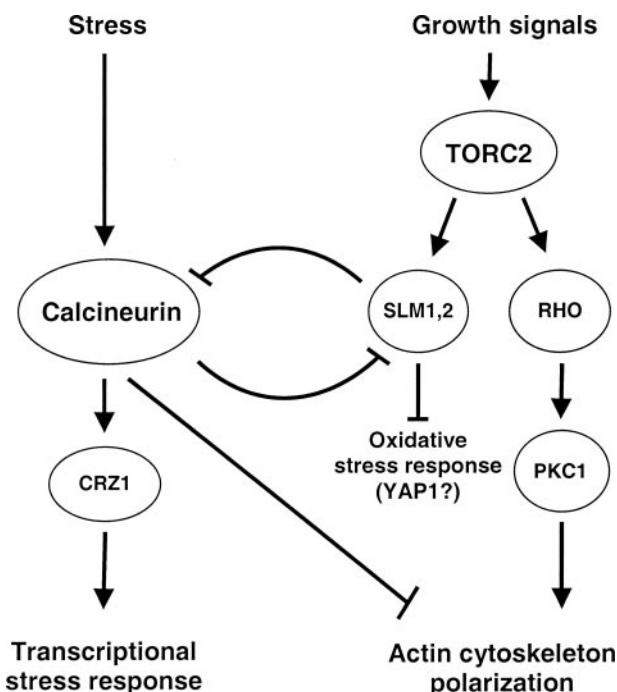


FIGURE 6. Model for mutual antagonism TORC2 and calcineurin signaling. Stress induces a rise in cytoplasmic calcium that activates calcineurin. Activated calcineurin dephosphorylates the SLM proteins and CRZ1. Calcineurin-mediated dephosphorylation of SLM disrupts signaling to the oxidative stress response and possibly other targets. In the absence of stress, TORC2 signals through the SLMs to control calcineurin and the oxidative stress response. SLM1,2 is required to block calcineurin signaling in normal growth conditions.

polarization via inhibition of calcineurin. The observation that the *SLM1^{ΔC14}* mutation has no effect on the actin cytoskeleton (data not shown) is further evidence for this notion. Although not shown in our model, the pleckstrin homology domain-containing SLM proteins also respond to the phosphatidylinositol-4-phosphate 5-kinase MSS4 (13, 14).

Is the mutual antagonism of calcineurin and TORC2-SLM direct or indirect? The observations that calcineurin binds the SLMs, and that calcineurin dephosphorylates SLM1 *in vivo* and *in vitro* suggest that calcineurin inhibits TORC2-SLM signaling by acting on SLM directly. The mechanism of inhibition in the other direction by which TORC2-SLM inhibits calcineurin is less clear. It seems unlikely that TORC2-SLM inhibits calcineurin directly because SLM1 in the *SLM1^{ΔC14} slm2* mutant is unable to bind calcineurin, and yet this mutant grows normally and is thus still able to inhibit calcineurin. Furthermore, the observation that the *SLM1^{ΔC14} slm2* mutant responds normally to salt stress (*i.e.* calcineurin activation) suggests that SLM dephosphorylation by calcineurin is not required to activate calcineurin. How might TORC2-SLM inhibit calcineurin indirectly? We were unable to detect a change in the concentration of cytoplasmic calcium in *tor2* and *avo3* mutants, as assayed with a calcium-specific dye (Fluo-3 AM) (data not shown), suggesting that TORC2-SLM inhibits calcineurin by a mechanism other than the modulation of cytoplasmic calcium. Another possibility is that TORC2-SLM modulates the activity of the calcineurin regulator RCN1 (26). Indeed, *RCN1* transcription is up-regulated in the *tor2^{ts}* mutant at nonpermissive

temperature (Fig. 1). The mechanism by which TORC2-SLM inhibits calcineurin remains to be determined.

We present evidence that TORC2 inhibits calcineurin/CRZ1-dependent transcription and the oxidative stress response. Furthermore, TORC2 seems to control these two new readouts independently of the previously characterized RHO-PKC1-MPK1 effector pathway (Fig. 6). Although TORC1 has been known for some time to control several cellular processes via different effector pathways, TORC2 was thought to signal only to the actin cytoskeleton and only via the RHO-PKC-MPK1 pathway. TORC2, like TORC1, now appears to have multiple effectors and targets. The complexity of TORC2 signaling has been underestimated possibly because TORC2 is rapamycin-insensitive, and studies on TOR function have usually relied on rapamycin to inhibit TOR signaling. Interestingly, an important aspect of TORC1 signaling in both yeast and mammalian cells is the inhibition of type 2A and type 2A-related phosphatases (27). Our observations suggest that TORC2 also signals via inhibition of a phosphatase, in this case calcineurin.

How does TORC2-SLM signaling inhibit the oxidative stress response? Yokoyama *et al.* (28) have suggested that YAP1, a transcription factor mediating the oxidative stress response, is controlled by calcineurin. Thus, an appealing model is that TORC2-SLM signaling inhibits the oxidative stress response by inhibiting YAP1. In the absence of stress, SLM is phosphorylated and bound to TORC2 and could thereby serve as an adaptor presenting YAP1 to TORC2 for phosphorylation and inhibition. Alternatively, as YAP1 is regulated at the level of nuclear localization, phosphorylated SLM could simply bind and sequester YAP1. In response to stress, calcineurin dephosphorylates SLM and possibly YAP1, leading to activation of YAP1. Interestingly, at least three CRZ1-independent YAP1 target genes (*CTT1*, *ARG4*, and *LAP4*) are up-regulated in the *tor2^{ts}* mutant at nonpermissive temperature (www.ncbi.nlm.nih.gov/geo/; accession number GSE1814). It is also interesting to note that TOR controls nuclear localization of several stress-related transcription factors, including *GLN3*, *GAT1*, *MSN2/4*, *RTG1*, *RTG3*, and as shown here, *CRZ1* (15, 29, 30).

Does mTOR inhibit calcineurin in mammalian cells? mTOR promotes skeletal myotube hypertrophy in response to insulin-like growth factor-1, and this effect is enhanced by the calcineurin inhibitor cyclosporin A (31). Furthermore, mTORC2 mediates actin polymerization in mammalian cells (32, 33), and calcineurin induces F-actin destabilization in dendritic spines (34). Thus, mTORC2 may inhibit calcineurin also in mammalian cells. mTORC2 signaling, which like TORC2 signaling in yeast is rapamycin-insensitive, probably has a broader role in the control of cell growth than commonly appreciated.

Acknowledgment—We thank Paul Jenoe for help in protein analysis.

REFERENCES

- Loewith, R., Jacinto, E., Wullschleger, S., Lorberg, A., Crespo, J. L., Bonenfant, D., Oppliger, W., Jenoe, P., and Hall, M. N. (2002) *Mol. Cell* **10**, 457–468
- Wedaman, K. P., Reinke, A., Anderson, S., Yates, J., 3rd, McCaffery, J. M., and Powers, T. (2003) *Mol. Biol. Cell* **14**, 1204–1220
- Wullschleger, S., Loewith, R., and Hall, M. N. (2006) *Cell* **124**, 471–484
- Schmidt, A., Bickel, M., Beck, T., and Hall, M. N. (1997) *Cell* **88**, 531–542
- Helliwell, S. B., Schmidt, A., Ohya, Y., and Hall, M. N. (1998) *Curr. Biol.* **8**, 1211–1214
- Cyert, M. S. (2001) *Annu. Rev. Genet.* **35**, 647–672
- Stathopoulos, A. M., and Cyert, M. S. (1997) *Genes Dev.* **11**, 3432–3444
- Matheos, D. P., Kingsbury, T. J., Ahsan, U. S., and Cunningham, K. W. (1997) *Genes Dev.* **11**, 3445–3458
- Mendizabal, I., Rios, G., Mulet, J. M., Serrano, R., and de Larrinoa, I. F. (1998) *FEBS Lett.* **425**, 323–328
- Mizunuma, M., Hirata, D., Miyahara, K., Tsuchiya, E., and Miyakawa, T. (1998) *Nature* **392**, 303–306
- Shitamukai, A., Hirata, D., Sonobe, S., and Miyakawa, T. (2004) *J. Biol. Chem.* **279**, 3651–3661
- Uetz, P., Giot, L., Cagney, G., Mansfield, T. A., Judson, R. S., Knight, J. R., Lockshon, D., Narayan, V., Srinivasan, M., Pochart, P., Qureshi-Emili, A., Li, Y., Godwin, B., Conover, D., Kalbfleisch, T., Vijayadamar, G., Yang, M., Johnston, M., Fields, S., and Rothberg, J. M. (2000) *Nature* **403**, 623–627
- Audhya, A., Loewith, R., Parsons, A. B., Gao, L., Tabuchi, M., Zhou, H., Boone, C., Hall, M. N., and Emr, S. D. (2004) *EMBO J.* **23**, 3747–3757
- Fadri, M., Daquinag, A., Wang, S., Xue, T., and Kunz, J. (2005) *Mol. Biol. Cell* **16**, 1883–1900
- Beck, T., and Hall, M. N. (1999) *Nature* **402**, 689–692
- Sherman, F. (1991) *Methods Enzymol.* **194**, 3–21
- Wullschleger, S., Loewith, R., Oppliger, W., and Hall, M. N. (2005) *J. Biol. Chem.* **280**, 30697–30704
- Longtine, M. S., McKenzie, A., 3rd, Demarini, D. J., Shah, N. G., Wach, A., Brachat, A., Philippsen, P., and Pringle, J. R. (1998) *Yeast* **14**, 953–961
- Helliwell, S. B., Howald, I., Barbet, N., and Hall, M. N. (1998) *Genetics* **148**, 99–112
- Martin, D. E., Demougin, P., Hall, M. N., and Bellis, M. (2004) *BMC Bioinformatics* **5**, 148
- Schmitt, M. E., Brown, T. A., and Trumpower, B. L. (1990) *Nucleic Acids Res.* **18**, 3091–3092
- Heath, V. L., Shaw, S. L., Roy, S., and Cyert, M. S. (2004) *Eukaryot. Cell* **3**, 695–704
- Schmelzle, T., Beck, T., Martin, D. E., and Hall, M. N. (2004) *Mol. Cell Biol.* **24**, 338–351
- Yoshimoto, H., Saltsman, K., Gasch, A. P., Li, H. X., Ogawa, N., Botstein, D., Brown, P. O., and Cyert, M. S. (2002) *J. Biol. Chem.* **277**, 31079–31088
- Stathopoulos-Gerontides, A., Guo, J. J., and Cyert, M. S. (1999) *Genes Dev.* **13**, 798–803
- Kingsbury, T. J., and Cunningham, K. W. (2000) *Genes Dev.* **14**, 1595–1604
- Jacinto, E., and Hall, M. N. (2003) *Nat. Rev. Mol. Cell Biol.* **4**, 117–126
- Yokoyama, H., Mizunuma, M., Okamoto, M., Yamamoto, J., Hirata, D., and Miyakawa, T. (2006) *EMBO Rep.* **7**, 519–524
- Komeili, A., Wedaman, K. P., O'Shea, E. K., and Powers, T. (2000) *J. Cell Biol.* **151**, 863–878
- Crespo, J. L., Powers, T., Fowler, B., and Hall, M. N. (2002) *Proc. Natl. Acad. Sci. U. S. A.* **99**, 6784–6789
- Rommel, C., Bodine, S. C., Clarke, B. A., Rossman, R., Nunez, L., Stitt, T. N., Yancopoulos, G. D., and Glass, D. J. (2001) *Nat. Cell Biol.* **3**, 1009–1013
- Jacinto, E., Loewith, R., Schmidt, A., Lin, S., Ruedig, M. A., Hall, A., and Hall, M. N. (2004) *Nat. Cell Biol.* **6**, 1122–1128
- Sarbassov, D. D., Ali, S. M., Kim, D. H., Guertin, D. A., Latek, R. R., Erdjument-Bromage, H., Tempst, P., and Sabatini, D. M. (2004) *Curr. Biol.* **14**, 1296–1302
- Halpain, S., Hipolito, A., and Saffer, L. (1998) *J. Neurosci.* **18**, 9835–9844